© 2018. Published by The Company of Biologists Ltd | Journal of Cell Science (2018) 131, jcs207522. doi:10.1242/jcs.207522

SHORT REPORT

Yeast cells contain a heterogeneous population of peroxisomes that segregate asymmetrically during cell division

Sanjeev Kumar Choudhry*, Rinse de Boer and Ida J. van der Klei‡

ABSTRACT

Here, we used fluorescence microscopy and a peroxisome-targeted tandem fluorescent protein timer to determine the relative age of peroxisomes in yeast. Our data indicate that yeast cells contain a heterogeneous population of relatively old and young peroxisomes. During budding, the peroxisome retention factor inheritance of peroxisomes protein 1 (Inp1) selectively associates to the older organelles, which are retained in the mother cells. Inp2, a protein required for transport of peroxisomes to the bud, preferentially associates to younger organelles. Using a microfluidics device, we demonstrate that the selective segregation of younger peroxisomes to the buds is carefully maintained during multiple budding events. The replicative lifespan of mother cells increased upon deletion of *INP2*, which resulted in the retention of all organelles in mother cells. These data suggest that, in wild-type yeast, transport of aged and deteriorated peroxisomes to the bud is prevented, whereas the young and vital organelles are preferably transported to the newly forming buds.

KEY WORDS: Peroxisome, Organelle inheritance, Yeast, Replicative lifespan, Organelle, Peroxisome inheritance

INTRODUCTION

Eukaryotic cells contain membrane-bound compartments called organelles that carry out specific functions. Among them, peroxisomes are organelles bound by a single membrane that are present in almost all eukaryotic cells. These physiologically important organelles harbor a large variety of metabolic and non-metabolic functions, depending on the organism, its developmental stage and the tissue. A common peroxisome function is hydrogen peroxide metabolism (Kohlwein et al., 2013; Wanders and Waterham, 2006). Along with mitochondria, peroxisomes contribute to reactive oxygen species homeostasis and are thought to play an important role in cellular ageing (Lefevre et al., 2015; Manivannan et al., 2012; Titorenko and Terlecky, 2011).

Two modes of peroxisome proliferation have been proposed, namely multiplication by fission of pre-existing organelles and *de novo* formation from the endoplasmic reticulum. Although controversy remains about the extent to which each of these two mechanisms contributes to the total cellular peroxisome population in different organisms, data obtained in the yeast species *Hansenula polymorpha* (Nagotu et al., 2008) and *Saccharomyces cerevisiae* (Motley and Hettema, 2007) indicate that peroxisome fission is the major pathway in these organisms.

According to the so-called growth and division model of peroxisome proliferation (Lazarow and Fujiki, 1985), a pre-existing peroxisome grows by incorporating newly synthesized membrane and matrix constituents until it reaches a mature size. Subsequently, this organelle divides, a process that involves the three consecutive steps of elongation, constriction and membrane scission (Lazarow and Fujiki, 1985; Motley and Hettema, 2007). Potentially, peroxisomes can divide symmetrically or asymmetrically. Symmetric division of peroxisomes leads to an equal distribution of the components of the mother organelle in the two daughter organelles. Upon growth, these daughter organelles have similar fractions of proteins originating from the mother organelle and of newly incorporated proteins. In contrast, asymmetric division of peroxisomes produces dissimilar organelles. Upon further growth of the smaller organelles, the result is one organelle containing predominantly proteins originating from the mother organelle and a second organelle that is mainly composed of newly synthesized components.

It has been suggested that peroxisomes in mammalian cells divide asymmetrically (Schrader et al., 2012), resulting in larger, mature mother organelles in conjunction with smaller daughter peroxisomes. Fluorescence microscopy data from yeast indicate that peroxisomes are heterogeneous with respect to the distribution of certain peroxisomal membrane proteins (Cepińska et al., 2011; Yofe et al., 2016). However, it is unknown whether the organelle population is also heterogeneous with respect to age.

Using a tandem fluorescent protein timer (Khmelinskii et al., 2012), we studied the heterogeneity of peroxisomes in *S. cerevisiae*. This approach can distinguish between relatively young and old peroxisomes. Our data indicate that, within one cell, peroxisomes differ with respect to the age of their matrix protein content. In addition, we observed that the relatively old organelles are retained in the mother cells during yeast budding, whereas the younger ones are transported to the buds. This careful segregation of older and younger organelles is maintained during multiple budding events. Interestingly, the replicative lifespan (RLS) of mother cells of an *inp2* deletion strain was longer than that of a wild-type control. In this strain, both the older and newer organelles are retained in the mother cells. Our data suggest that in wild-type yeast cells the older, possibly deteriorated, organelles are retained in the mother cell, whereas the younger more vital organelles are preferentially transported to the buds.

RESULTS AND DISCUSSION

Yeast cells contain a heterogeneous population of peroxisomes

To determine the relative age of the peroxisomal matrix content, we used a fusion protein consisting of DsRed1 and superfolder GFP

Molecular Cell Biology, Groningen Biomolecular Sciences and Biotechnology Institute, University of Groningen, P.O. Box 11103, 9700CC, Groningen, The Netherlands.
*Present address: Center for Infectious Disease Research, Seattle, WA 98109, USA.

‡Author for correspondence (i.j.van.der.klei@rug.nl)

S.K.C., 0000-0003-2685-9940; I.J.V.d.K., 0000-0001-7165-9679

Received 22 June 2017; Accepted 13 December 2017

Journal of Cell Science (2018) 131, jcs207522. doi:10.1242/jcs.207522

(sfGFP) (Khmelinskii et al., 2012) with the peroxisomal targeting signal –SKL at the extreme C-terminus (Fig. 1A), placed under control of the constitutive promoter of the glyceraldehyde 3-phosphate dehydrogenase gene (p*THD3*). DsRed1 has a very long maturation time (half-life ∼11 h) (Campbell et al., 2002), whereas sfGFP maturation takes only a few minutes (Pédelacq et al., 2006). Upon import of this fusion protein into peroxisomes, sfGFP immediately shows green fluorescence, whereas the red fluorescence gradually increases with time. Thus, the ratio of the fluorescence intensities of DsRed1 to sfGFP can serve as a measure of the age of peroxisomal matrix protein content. If peroxisomes divide symmetrically, resulting in daughter organelles that have a similar capacity to import matrix proteins, all organelles within one cell are expected to show a similar ratio of green to red fluorescence (Fig. 1B). However, asymmetric peroxisome fission probably results in a heterogeneous population of organelles, with a range of DsRed1/sfGFP fluorescence intensity ratios (Fig. 1B).

As shown in Fig. 1C, fluorescence microscopy of glucose-grown cells revealed multiple green fluorescent spots per cell, whereas only a subset of organelles also showed bright red fluorescence (Fig. 1C). We measured fluorescence intensities of DsRed1 and sfGFP on individual peroxisomes, which were normalized to the total fluorescence intensity of the respective fluorophore in the cell. Under our experimental conditions, all peroxisomes showed both green and red fluorescence (Fig. S1). As expected, correlation between fluorescence intensities of these fluorophores on individual peroxisomes showed no linear relationship. Instead, peroxisomes with relatively low sfGFP fluorescence intensities showed much lower DsRed1 intensities than expected for a linear relationship (Fig. S1). This result shows that indeed peroxisomes occur in cells, which contain newly synthesized DsRed1–sfGFP fusion protein, of which the DsRed1 portion of this fusion is not yet fully mature. To capture the whole range of heterogeneity, we did not use any fluorescence intensity cutoffs in our quantification except for removal of background fluorescence. As expected, quantification of the DsRed1/sfGFP fluorescence intensity ratios on individual peroxisomes revealed a large heterogeneity in glucose-grown cells (Fig. 1D). A similar heterogeneity was observed when cells were grown on oleic acid, a condition that induces peroxisome proliferation (Fig. 1E).

The heterogeneity was not caused by proteolytic degradation of the fusion protein, because western blot analysis indicated that almost all protein was present in the full-length form (Fig. S2). The

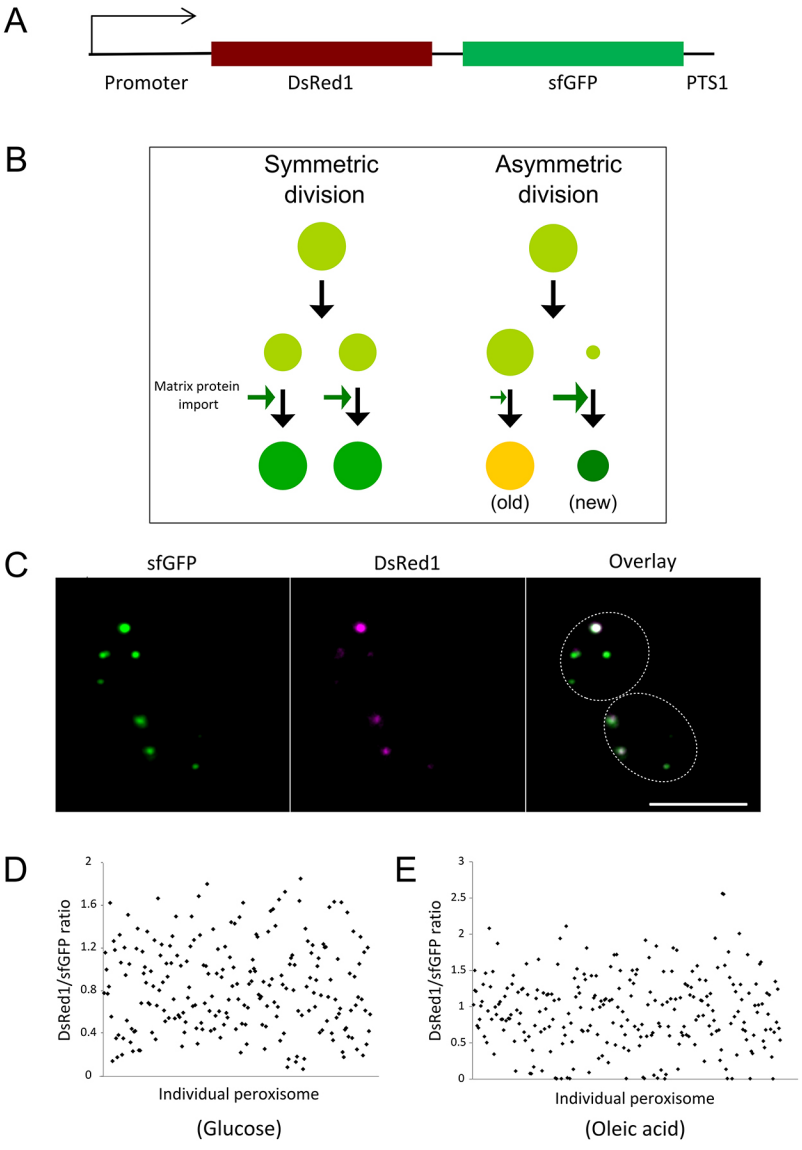

Fig. 1. Heterogeneity of peroxisomes. (A) Scheme of the peroxisomal tandem fluorescent protein containing slow maturing DsRed1 and fast maturing sfGFP. (B) Hypothetical models of two possible modes of peroxisome proliferation and the corresponding predicted distribution of new and old matrix proteins. Dark green represents new matrix protein, yellow is old matrix protein. The thickness of the green arrows represents the extent of matrix protein import into peroxisomes. (C) Image of yeast cells producing the DsRed1–sfGFP–SKL fusion protein. GFP fluorescence is in green and DsRed1fluorescence is in magenta; co-localization is shown in white. All organelles show green fluorescence, whereas only a subset also contains bright red fluorescence. Scale bar: 5 µm. (D,E) Fluorescence intensity ratios of DsRed1 to sfGFP on individual peroxisomes in cells grown for 16 h on medium containing glucose (D) or oleic acid (E). Fluorescence intensity of sfGFP (or DsRed1) of each peroxisome was normalized by dividing by the total intensity of sfGFP (or DsRed1) in that cell.

Journal of Cell Science (2018) 131, jcs207522. doi:10.1242/jcs.207522

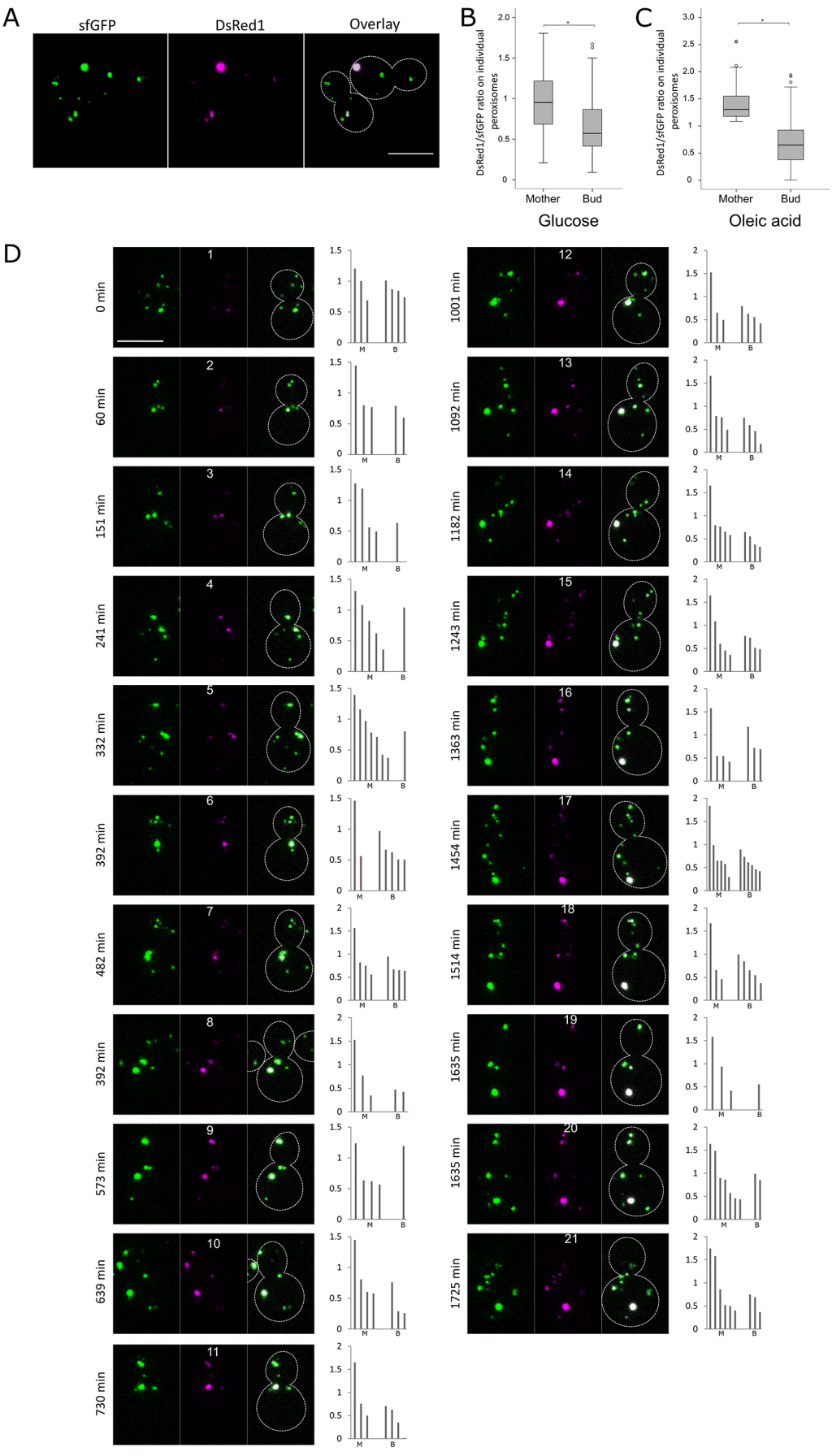

Fig. 2. Peroxisome inheritance. (A) Peroxisomes marked with the fusion protein DsRed1–sfGFP–SKL in budding *S. cerevisiae* cells. (B,C) Box plots shows the DsRed1/sfGFP fluorescence intensity ratio for individual peroxisomes in mother cells and buds in glucose-grown dividing cells (n=47) (B) or oleic acid grown dividing cells (n=49) (C). *P<0.0001 by two-tailed Student's t-test. (D) Single cell analysis of peroxisome inheritance for 21 consecutive cell divisions using a microfluidics chip. Each image shows peroxisome distribution during one budding event. Numbers above images indicate the cell division number. Bar chart next to each image shows the DsRed1/sfGFP fluorescence intensity ratio for individual peroxisomes in mother cell (M) or bud (B). Fluorescence intensity of sfGFP (or DsRed1) on each peroxisome was normalized to the total intensity of sfGFP (or DsRed1) in the dividing cell during each division. Scale bars: 5 µm.

Journal of Cell Science (2018) 131, jcs207522. doi:10.1242/jcs.207522

observed heterogeneity confirms that peroxisomes divide asymmetrically in both glucose- and oleic acid-grown yeast cells,.

Mature peroxisomes are retained in the mother cell, whereas nascent peroxisomes segregate to the bud

Next, we investigated the fate of nascent and mature organelles during growth of cells on glucose. Fluorescence microscopy of a strain constitutively producing DsRed1–sfGFP–SKL revealed that peroxisomes with high red fluorescence were generally localized in the mother cells, whereas organelles that showed low or no red fluorescence were more abundant in the buds (Fig. 2A). This was confirmed by a significantly higher ratio of DsRed1 to sfGFP fluorescence intensity on individual peroxisomes in mother cells relative to those present in developing buds (Fig. 2B). Furthermore, the fluorescence intensity ratio of total cellular DsRed1 to sfGFP was also higher in the mother cells relative to the buds, confirming that organelles with older peroxisomal matrix proteins are preferentially retained in the mother cells (Fig. S3A). Similar results were obtained when cells were grown on oleic acid (Fig. 2C; Fig. S3B).

S. cerevisiae mother cells typically produce approximately 25 buds before they die. Using a microfluidics device, we checked whether the observed asymmetry in peroxisome inheritance was maintained during multiple consecutive budding events of an individual mother cell. In this experimental set-up, individual mother cells trapped in a microfluidics device are imaged by fluorescence microscopy during multiple budding events, while the daughter cells are continuously removed by a flow of fresh medium (Lee et al., 2012). A representative example is shown in Fig. 2D, where the peroxisome inheritance of one individual yeast mother cell is monitored during 21 consecutive budding events (total time of imaging approximately 30 h). This experiment shows that the peroxisome with the highest DsRed1/sfGFP fluorescence intensity ratio was always retained in the mother cell, whereas the other organelles were segregated between mother and daughter cells (Fig. 2D).

Our results indicate that retention of older peroxisomes in mother cells and segregation of nascent peroxisomes to buds is carefully controlled during the entire replicative lifespan of the mother cells. The retention of the older peroxisomes in the mother cell is most probably independent of their larger size because peroxisomes measure up to 0.2 µm in diameter in glucose-grown *S. cerevisiae* cells (Veenhuis et al., 1987) whereas the diameter of the bud neck is about 1 µm (Bertin et al., 2012). Hence, even the largest organelles can easily pass through the bud neck. Moreover, if the largest peroxisomes became stuck at the bud neck because of their size, they would accumulate close to the bud neck, which was never observed.

Inheritance of peroxisomes protein 1 (Inp1) is a peroxisomal membrane protein that plays a role in peroxisome retention in the mother cell, whereas Inp2 is required to transport peroxisomes to the yeast bud via actin filaments (Fagarasanu et al., 2005, 2006). Localization of both proteins in cells of strains producing DsRed1–SKL revealed that Inp1–GFP was mainly present in mother cells on peroxisomes with high DsRed1 intensities (Fig. 3A), whereas Inp2–GFP was enriched in daughter cells on peroxisomes with low DsRed1 fluorescence intensity (Fig. 3B).

Quantification of GFP fluorescent spots in the dividing cells showed that Inp1–GFP spots were abundant in the mother cells whereas Inp2–GFP spots were prevalent in buds (Fig. 3C). Moreover, total GFP fluorescence intensity quantification in the mothers and buds further confirmed that Inp1–GFP fluorescence

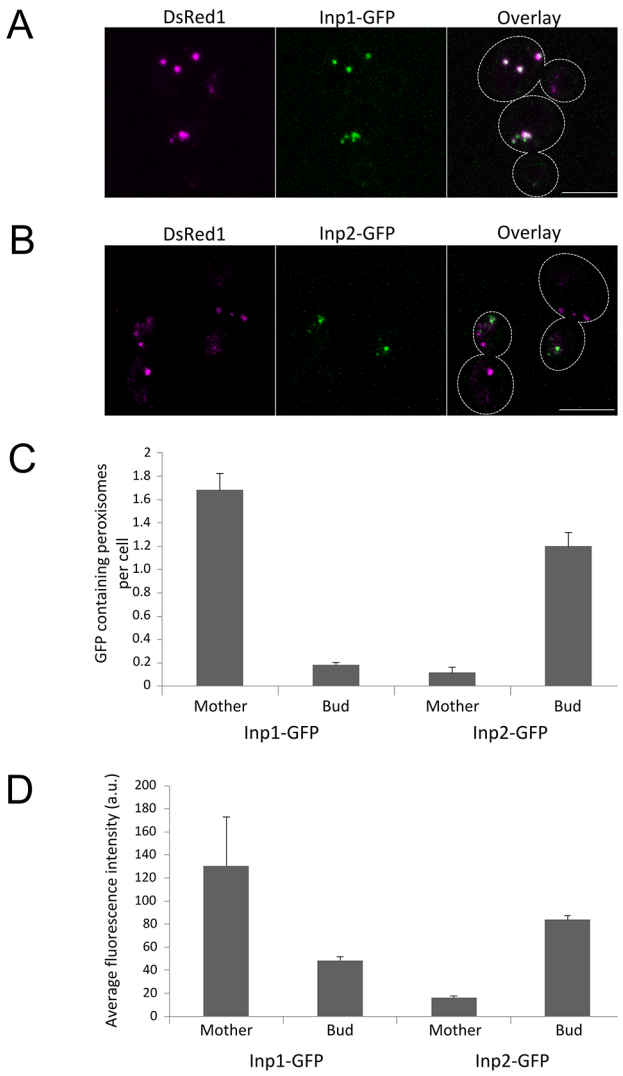

Fig. 3. Distribution of Inp1 and Inp2 on peroxisomes. (A) Fluorescence microscopy image showing the distribution of Inp1–GFP on peroxisomes marked with DsRed1–SKL (B) Fluorescence microscopy images showing the distribution of Inp2–GFP on peroxisomes marked with DsRed1–SKL. (C) Quantification of Inp1–GFP and Inp2–GFP spots in the mother cell and bud. (D) Quantification of average fluorescence intensity of Inp1–GFP and Inp2–GFP in the mother cell and bud (n= 60; error bar represents standard deviation of mean). Both Inp1–GFP and Inp2–GFP were produced under control of their endogenous promoters. Scale bars: 5 µm.

intensity was higher in mother cells, whereas Inp2–GFP intensity was higher in buds (Fig. 3D).

These observations are in line with earlier observations in *S. cerevisiae* and *H. polymorpha*, which indicated that Inp1-containing peroxisomes are retained in mother cells, whereas organelles that move to the bud harbor Inp2 (Cepińska et al., 2011; Knoblach et al., 2013). We now show for the first time that Inp1 and Inp2, which both are produced in a cell cycle dependent way, associate with mature and nascent organelles, respectively. Inp1 is recruited to peroxisomes by the membrane protein Pex3, which is present on all organelles (Knoblach et al., 2013). Possibly, the levels of Pex3 increase in time on the older organelles, thus increasing the capacity of the organelles to bind Inp1. Inp2 is an integral peroxisomal membrane protein. How this protein preferably inserts into the membranes of the younger organelles is unknown.

Journal of Cell Science (2018) 131, jcs207522. doi:10.1242/jcs.207522

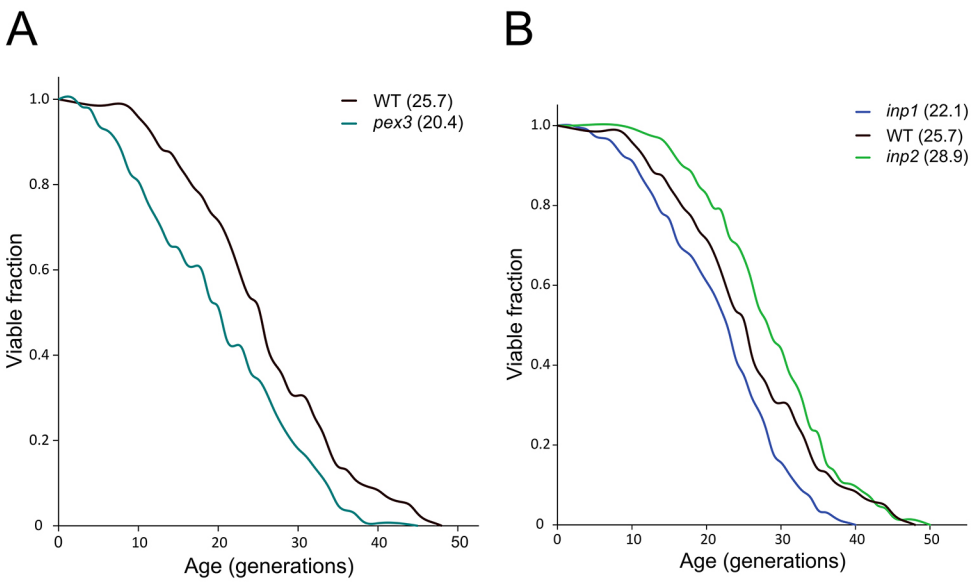

Fig. 4. *PEX3* and *INP1* deletion reduces yeast replicative lifespan. (A,B) Replicative lifespan of wild-type (A), *pex3* (A), *inp1* (B) and *inp2* (B) cells. Replicative lifespan was measured using a microfluidics device. Mean RLS for wild-type 25.7, for *pex3* 20.4, for *inp1* 22.1 and for *inp2* 28.9. Number of cells counted (*n*) was 144 for wild-type, 166 for *pex3*, 192 for *inp1* and 145 for *inp2*.

A possible mechanism is that higher curvature of the membranes in the smaller, younger organelles plays a role.

The enhanced level of Inp1 on older peroxisomes enables effective retention of these organelles in the mother cells by not allowing their transfer to the daughter cell. By contrast, the presence of Inp2 on the nascent organelles preferentially transfers these peroxisomes to the bud. This asymmetry could prevent transfer of damaged, mature organelles to newly formed buds.

Interfering in normal peroxisome partitioning during yeast budding affects the replicative lifespan

To test the physiological relevance of the careful partitioning of mature and nascent organelles between mother and daughter cells, we analyzed whether interfering in this process affects the RLS of mother cells.

First, our studies revealed that intact peroxisomes are important for yeast RLS because *pex3* cells, which lack functional peroxisomes, show a reduced RLS relative to wild-type controls (Fig. 4A; mean RLS of *pex3* cells is 20.4, compared with 25.7 for the wild-type control).

Next, we analyzed *inp1* and *inp2* mutant strains. In cells lacking *INP1*, all peroxisomes are transported to the developing buds, leaving mother cells devoid of peroxisomes. Conversely, deletion of *INP2* results in the retention of all organelles in the mother cell and the formation of buds without peroxisomes. In *inp1* cells, peroxisome numbers are decreased (Fagarasanu et al., 2005), whereas *inp2* cells show a heterogeneity of peroxisome numbers, with some cells containing more peroxisomes and others less than in wild-type cells (Fagarasanu et al., 2006). As shown in Fig. 4B, the RLS of *inp1* cells is reduced relative to the wild-type control, whereas that of *inp2* cells is enhanced. Obviously, the loss of all peroxisomes in *inp1* mother cells decreases the lifespan of these cells. Conversely, our data suggest that the retention of all organelles in the mother cells positively affects the RLS.

It has been suggested that, in *S. cerevisiae*, peroxisomes are not important when cells are grown on glucose, because peroxisome-deficient mutants normally grow on medium containing glucose. However, our data show that glucose-grown *pex3* cells, which do not contain functional peroxisomes, have a shorter RLS than wild-type controls. Similarly, mother cells of an *INP1*-deficient strain, which are unable to retain peroxisomes, show a reduced RLS in glucose-containing medium. These observations indicate that functional peroxisomes are important for the RLS of glucose-grown yeast cells. The finding that retention of all peroxisomes in mother cells of the *inp2* strain has a positive effect on yeast RLS further supports this conclusion. Possibly, enhanced levels of peroxisomal catalase in mother cells of the *inp2* mutant strain contribute to reduced levels of reactive oxygen species, which may enhance the RLS. However, other as-yet-unknown peroxisome-bound metabolic or non-metabolic functions might also contribute to extension of the RLS (Fransen et al., 2012).

MATERIALS AND METHODS

Strains and growth conditions

The *S. cerevisiae* strains used in this study are listed in Table S1. Cells were grown at 30°C on mineral medium (MM) (Van Dijken et al., 1976) containing 0.25% ammonium sulfate and 2% glucose or 0.1% oleic acid. MM was supplemented with the required amino acids or uracil to a final concentration of 20 µg/ml (histidine and methionine) or 30 µg/ml (leucine, lysine and uracil). For growth on agar plates, YPD medium (1% yeast extract, 1% peptone, 1% glucose) was supplemented with 2% agar. For selection of zeocin- or nourseothricin-resistant transformant, YPD plates containing 200 µg/ml zeocin (Invitrogen) or 100 µg/ml nourseothricin (Werner BioAgents) were used. To select transformants based on amino acid prototrophy, yeast nitrogen base (YNB) plates without amino acids (Difco; BD), containing 1% glucose and 2% agar, was used with the appropriate amino acids. For cloning purposes, *Escherichia coli* DH5α was used, which was cultured at 30°C on Luria–Bertani medium supplemented with the appropriate antibiotics.

Construction of *S. cerevisiae* strains

Yeast strains, plasmids and primers used in this study are listed in Tables S1, S2 and S3, respectively.

To construct pSAN02, *DsRED1* was amplified from pYM35 (Janke et al., 2004) using primers DsRED1-Fw and DsRed1-Rev, digested with *Bam*HI/*Hin*dIII and cloned into pSL34 (Lefevre et al., 2013), resulting in plasmid pP_{MET25}-DsRed1-SKL. Subsequently, DsRed1–SKL was amplified from pP_{MET25}-DsRed1-SKL using primers DsRED1-1 and DsRED1-2, digested with *Hin*dIII/*Sal*I and cloned into pHIPN4 (Saraya et al., 2012), resulting in plasmid pHIPN4-DsRed1-SKL. The *TDH3* promoter was amplified from *S. cerevisiae* genomic DNA using primers TDH3-4 and TDH3-5, digested with *Not*I/*Hin*dIII and cloned into pHIPN4-DsRed1-SKL, which resulted in plasmid pP_{TDH3}-DsRed1-SKL (pSAN02). pSAN02 was linearized using MfeI and integrated in the *THD3* promoter region of the *S. cerevisiae* genome.

For construction of a plasmid encoding a fusion protein of DsRed1 and sfGFP containing the peroxisomal targeting signal 1 (PTS1) sequence –SKL at the extreme C-terminus, an mCherry–sfGFP fragment was first amplified from pMaM17 (Khmelinskii et al., 2012) using primer pair MC.sfGFP-Fw/MC.sfGFP-Rev. This PCR fragment was digested with *Aat*II/*Xho*I and cloned into pSL33, resulting in plasmid pP_{MET25}-mCherry-sfGFP-SKL. From this plasmid, an mCherry–sfGFP–SKL fragment was amplified using primer pair MC.sfGFP-1/MC.sfGFP-2 and a *Hin*dIII/*Sal*I fragment was cloned into pHIPZ4 (Salomons et al., 2000), resulting in pHIPZ-mCherry-sfGFP-SKL. The DsRed1 was amplified from pYM35 using DsRed1.*Hin*dIII_F and DsRED2.OL; sfGFP–SKL was amplified from pHIPZ-mCherry-sfGFP-SKL using primers sfGFP.DsRED1.OL and sfGFP_R. Both fragments were joined together by overlap PCR and the *Hin*dIII/*Sal*I fragment cloned into pSAN02, resulting in plasmid pP_{TDH3}-DsRed1-sfGFP-SKL (pSAN03). Plasmid pSAN03 was linearized by restriction enzyme MfeI and integrated into the *S. cerevisiae* genome.

To construct pSL33, the P_{MET25}-DsRed-SKL-tcyc1 fragment was amplified from pUG34-DsRed-SKL (Kuravi et al., 2006) using primer pair DsRed-1/DsRed-2. The obtained PCR product was digested with *Kpn*I/*Xba*I and cloned into pBSII KS^+, resulting in pSL32. The nourseothricin resistance gene was amplified from pAG25 (Goldstein and McCusker, 1999) using primer pair Nat1.1/Nat1.2, digested with *Sac*II/*Kpn*I and cloned into pSL32, resulting in pSL33.

Fluorescence microscopy

Wide-field fluorescence images (Fig 1C; Fig 2A) were acquired using a 100×1.30 NA Plan-Neofluar objective (Carl Zeiss). These images were captured by an inverted microscope (Observer Z1; Carl Zeiss) using AxioVision software (Carl Zeiss) and a digital camera (CoolSNAP HQ^2; Photometrics). The GFP signal was visualized with a 470/40-nm band pass excitation filter, a 495-nm dichromatic mirror and a 525/50-nm band pass emission filter. DsRed fluorescence was visualized with a 546/12-nm bandpass excitation filter, a 560-nm dichromatic mirror and a 575–640-nm bandpass emission filter. For both DsRed1 and sfGFP image acquisition, an exposure time of 500 ms was used. Under these conditions, the samples were not overexposed and the fluorescence intensities of the fluorophores not saturated, as established by the maximum pixel intensity value.

Confocal images (Figs 2D, 3A,B) were acquired with a confocal microscope (LSM510; Carl Zeiss) equipped with photomultiplier tubes (Hamamatsu Photonics) and Zen 2009 software (Carl Zeiss). GFP fluorescence was visualized by excitation with a 488-nm argon ion laser (Lasos), and emission detected using a 500–550-nm band-pass emission filter. The DsRed signal was visualized by excitation with a 543-nm helium neon laser (Lasos) and emission was detected using a 565–615-nm bandpass emission filter.

Image analysis was performed using ImageJ software. For quantification, peroxisomes were first selected based on green fluorescence and then the fluorescence intensities of sfGFP and DsRed1 on each peroxisome were measured. The fluorescence intensity on each peroxisome was corrected by subtracting the background intensity from a region in the cell without peroxisomes. Moreover, fluorescence intensities of sfGFP and DsRed1 on individual peroxisomes in a cell were normalized by dividing by the total intensity (sum of all peroxisomes) of the respective fluorophore in the cell. The normalized fluorescence intensities on each peroxisome were used to calculate the DsRed1/sfGFP fluorescence intensity ratio.

To study peroxisome inheritance, a single cell microfluidic dissection device was used with a constant supply of mineral medium. Time-lapse images were acquired using the confocal microscope LSM510. The objective and microfluidic dissection device were kept at 30°C.

Replicative lifespan analysis

The RLS of yeast strains was measured using a microfluidics dissection device (Lee et al., 2012) at 30°C. Mineral medium supplemented with 2% glucose and appropriate amino acids (without yeast extract) was supplied at a flow rate of 5–7 µl/min throughout the experiment. Time-lapse bright field images were acquired every 30 min using a wide field inverted microscope (Observer Z1; Carl Zeiss). The number of buds produced by each cell was counted and the RLS curve obtained using Kaplan–Meier analysis.

Acknowledgements

We would like to thank Kevin Knoops and Arjen M. Krikken for helpful discussions.

Competing interests

The authors declare no competing or financial interests.

Author contributions

Conceptualization: S.K.C., I.J.v.d.K.; Methodology: S.K.C., I.J.v.d.K.; Validation: S.K.C., R.d.B.; Formal analysis: S.K.C., R.d.B., I.J.v.d.K.; Investigation: S.K.C., R.d.B.; Writing -original draft: S.K.C., I.J.v.d.K.; Writing - review & editing: S.K.C., I.J.v.d.K.; Supervision: I.J.v.d.K.; Funding acquisition: I.J.v.d.K.

Funding

S.K.C. is supported by the Netherlands Organization for Scientific Research (Nederlandse Organisatie voor Wetenschappelijk Onderzoek; NWO) (723.013.004) and I.J.v.d.K. by the Marie Curie Initial Training Network (European Commission) PERFUME (PERoxisome Formation, Function, Metabolism) grant (grant agreement number 316723).

Supplementary information

Supplementary information available online at
http://jcs.biologists.org/lookup/doi/10.1242/jcs.207522.supplemental

References

Bertin, A., McMurray, M. A., Pierson, J., Thai, L., McDonald, K. L., Zehr, E. A., García, G., Peters, P., Thorner, J. and Nogales, E. (2012). Three-dimensional ultrastructure of the septin filament network in Saccharomyces cerevisiae. *Mol. Biol. Cell* **23**, 423-432.

Campbell, R. E., Tour, O., Palmer, A. E., Steinbach, P. A., Baird, G. S., Zacharias, D. A. and Tsien, R. Y. (2002). A monomeric red fluorescent protein. *Proc. Natl. Acad. Sci. USA* **99**, 7877-7882.

Cepińska, M. N., Veenhuis, M., van der Klei, I. J. and Nagotu, S. (2011). Peroxisome fission is associated with reorganization of specific membrane proteins. *Traffic* **12**, 925-937.

Fagarasanu, M., Fagarasanu, A., Tam, Y. Y. C., Aitchison, J. D. and Rachubinski, R. A. (2005). Inp1p is a peroxisomal membrane protein required for peroxisome inheritance in Saccharomyces cerevisiae. *J. Cell Biol.* **169**, 765-775.

Fagarasanu, A., Fagarasanu, M., Eitzen, G. A., Aitchison, J. D. and Rachubinski, R. A. (2006). The peroxisomal membrane protein Inp2p is the peroxisome-specific receptor for the myosin V motor Myo2p of Saccharomyces cerevisiae. *Dev. Cell* **10**, 587-600.

Fransen, M., Nordgren, M., Wang, B. and Apanasets, O. (2012). Role of peroxisomes in ROS/RNS-metabolism: Implications for human disease. *Biochim. Biophys. Acta* **1822**, 1363-1373.

Goldstein, A. L. and McCusker, J. H. (1999). Three new dominant drug resistance cassettes for gene disruption in Saccharomyces cerevisiae. *Yeast* **15**, 1541-1553.

Janke, C., Magiera, M. M., Rathfelder, N., Taxis, C., Reber, S., Maekawa, H., Moreno-Borchart, A., Doenges, G., Schwob, E., Schiebel, E. et al. (2004). A versatile toolbox for PCR-based tagging of yeast genes: new fluorescent proteins, more markers and promoter substitution cassettes. *Yeast* **21**, 947-962.

Khmelinskii, A., Keller, P. J., Bartosik, A., Meurer, M., Barry, J. D., Mardin, B. R., Kaufmann, A., Trautmann, S., Wachsmuth, M., Pereira, G. et al. (2012). Tandem fluorescent protein timers for in vivo analysis of protein dynamics. *Nat. Biotechnol.* **30**, 708-714.

Knoblach, B., Sun, X., Coquelle, N., Fagarasanu, A., Poirier, R. L. and Rachubinski, R. A. (2013). An ER-peroxisome tether exerts peroxisome population control in yeast. *EMBO J.* **32**, 2439-2453.

Kohlwein, S. D., Veenhuis, M. and van der Klei, I. J. (2013). Lipid droplets and peroxisomes: key players in cellular lipid homeostasis or a matter of fat–store 'em up or burn 'em down. *Genetics* **193**, 1-50.

Kuravi, K., Nagotu, S., Krikken, A. M., Sjollema, K., Deckers, M., Erdmann, R., Veenhuis, M. and van der Klei, I. J. (2006). Dynamin-related proteins Vps1p and Dnm1p control peroxisome abundance in Saccharomyces cerevisiae. *J. Cell Sci.* **119**, 3994-4001.

Lazarow, P. B. and Fujiki, Y. (1985). Biogenesis of peroxisomes. *Annu. Rev. Cell Biol.* **1**, 489-530.

Lee, S. S., Vizcarra, I. A., Huberts, D. H. E. W., Lee, L. P. and Heinemann, M. (2012). Whole lifespan microscopic observation of budding yeast aging through a microfluidic dissection platform. *Proc. Natl. Acad. Sci. USA* **109**, 4916-4920.

Lefevre, S. D., van Roermund, C. W., Wanders, R. J. A., Veenhuis, M. and van der Klei, I. J. (2013). The significance of peroxisome function in chronological aging of Saccharomyces cerevisiae. *Aging Cell* **12**, 784-793.

Lefevre, S. D., Kumar, S. and van der Klei, I. J. (2015). Inhibition of peroxisome fission, but not mitochondrial fission, increases yeast chronological lifespan. *Cell Cycle* **14**, 1698-1703.

Manivannan, S., Scheckhuber, C. Q., Veenhuis, M. and van der Klei, I. J. (2012). The impact of peroxisomes on cellular aging and death. *Mol. Cell. Oncol.* **2**, 50.

Motley, A. M. and Hettema, E. H. (2007). Yeast peroxisomes multiply by growth and division. *J. Cell Biol.* **178**, 399-410.

Nagotu, S., Saraya, R., Otzen, M., Veenhuis, M. and van der Klei, I. J. (2008). Peroxisome proliferation in *Hansenula polymorpha* requires Dnm1p which mediates fission but not de novo formation. *Biochim. Biophys. Acta* **1783**, 760-769.

Pédelacq, J.-D., Cabantous, S., Tran, T., Terwilliger, T. C. and Waldo, G. S. (2006). Engineering and characterization of a superfolder green fluorescent protein. *Nat. Biotechnol.* **24**, 79-88.

Salomons, F. A., Kiel, J. A. K. W., Faber, K. N., Veenhuis, M. and van der Klei, I. J. (2000). Overproduction of Pex5p stimulates import of alcohol oxidase and dihydroxyacetone synthase in a *Hansenula polymorpha* Pex14 null mutant. *J. Biol. Chem.* **275**, 12603-12611.

Saraya, R., Krikken, A. M., Kiel, J. A. K. W., Baerends, R. J. S., Veenhuis, M. and van der Klei, I. J. (2012). Novel genetic tools for *Hansenula polymorpha*. *FEMS Yeast Res.* **12**, 271-278.

Schrader, M., Bonekamp, N. A. and Islinger, M. (2012). Fission and proliferation of peroxisomes. *Biochim. Biophys. Acta* **1822**, 1343-1357.

Titorenko, V. I. and Terlecky, S. R. (2011). Peroxisome metabolism and cellular aging. *Traffic* **12**, 252-259.

Van Dijken, L. P., Otto, R. and Harder, W. (1976). Growth of *Hansenula polymorpha* in a methanol-limited chemostat. *Arch. Microbiol.* **111**, 137-144.

Veenhuis, M., Mateblowski, M., Kunau, W. H. and Harder, W. (1987). Proliferation of microbodies in Saccharomyces cerevisiae. *Yeast Chichester Engl.* **3**, 77-84.

Wanders, R. J. A. and Waterham, H. R. (2006). Biochemistry of mammalian peroxisomes revisited. *Annu. Rev. Biochem.* **75**, 295-332.

Yofe, I., Weill, U., Meurer, M., Chuartzman, S., Zalckvar, E., Goldman, O., Ben-Dor, S., Schütze, C., Wiedemann, N., Knop, M. et al. (2016). One library to make them all: streamlining the creation of yeast libraries via a SWAp-Tag strategy. *Nat. Methods* **13**, 371-378.